Wave Profile Modification in the Free Electron Laser With and Without a Waveguide

Amnon Fruchtman

Reprinted from
IEEE TRANSACTIONS ON PLASMA SCIENCE
Vol. 18, No. 3, June 1990

Wave Profile Modification in the Free Electron Laser With and Without a Waveguide

AMNON FRUCHTMAN

Abstract—**The modification of the transverse wave profile by the Free Electron Laser (FEL) interaction in the collective Raman regime is considered. We calculate the gain and find the transverse wave profile by solving for the eigenvalues and the actual eigenmodes of the system. When a waveguide is employed, a strong FEL interaction is shown to couple various vacuum waveguide modes, as was recently demonstrated by the Columbia group [23]. When no waveguide or cavity is present, we identify a coupling parameter which measures the strength of the interaction. We derive expressions for the gain for large and small values of the coupling parameter, corresponding to a strong optical guiding and large diffraction, respectively. Comparing the present results for the Raman regime with previous results for the strong-pump regime, we show that the gain scales differently in each case, depending upon both the regime of operation and on the beam geometry. Our linear analysis is valid when the signal is small, and is useful mainly when the gain is high prior to saturation.**

I. Introduction

THE MODIFICATION of the transverse profile of the electromagnetic wave in the Free Electron Laser (FEL) [1] is a subject of extensive theoretical [2]–[20] and experimental [21]–[23] study. It is hoped that the guiding of the amplified wave by the electron beam will eliminate the need for a cavity or a waveguide to confine the radiation. Also, the confinement of the wave profile to the electron beam volume increases the filling factor and thus strengthens the interaction. In this paper we examine how the FEL interaction of a cylindrical electron beam in the collective "Raman" regime modifies the radial profile of the wave in two situations: First, in the presence of a cylindrical waveguide; and secondly, when no such waveguide is present.

As in our previous papers [10], [16]–[18] and as has been done by several others [3]–[6], [14], [15], [30], we address this problem by formulating an eigenvalue problem for the transverse profile of the wave. The eigenfunctions are wave modes of a self-similar nature. They preserve their transverse profiles as they propagate along the FEL. The imaginary part of the eigenvalue determines the growth rate of the mode. The eigenvalue formulation is mostly useful to describe the interaction when the signal is small and the gain is high prior to saturation. The linear analysis is then valid and the wave grows exponentially. If one mode has a higher growth rate than all other modes, the growth rate of the most unstable mode is the actual growth rate of the wave, and the wave transverse profile is described by the profile of this mode. Thus solving for the eigenvalues and the actual eigenmodes of the system may directly yield the growth rate of the wave and its transverse profile, without the use of vacuum modes or of other systems of orthogonal functions. The eigenvalue formulation is not valid in the nonlinear regime. In the nonlinear regime, particle simulation is usually needed [2], [7], [9], [11], [21], [24] and because of mode coupling, probably more than one mode is needed to describe the wave profile. The linear eigenvalue formalism, however, could guide nonlinear particle simulation and the two methods could be complementary. A compressed version of our formalism with its application to the Columbia experiment [23], and with a comparison to the Columbia nonlinear simulations has appeared recently [26]. The results of our formalism and those of the Columbia simulations were found to be in good agreement. Here, we give a more detailed and rigorous version of the formalism. We also present the tool of energy integral and the asymptotic expressions of the gain and show additional effects such as the dependence of the wave profile on the waveguide radius and the wave guiding when a waveguide is not present.

We use a cold-fluid model to describe the electron dynamics. We do not address beam emittance, thermal spread, and betatron oscillations. The betatron oscillations introduce an effective thermal spread which limits the validity of the cold fluid model. Recently, Yu and Krinsky addressed betatron oscillations within an eigenvalue formulation [15].

In Section II we present the general formalism. Using the cold-fluid equations for the electron dynamics and the Maxwell equations for the waves, we analyze the interaction of an FEL which employs a cylindrical electron beam and which operates in the Raman regime. The governing equations are two decoupled second-order differential equations for two wave components. Their solutions may be coupled through the boundary conditions.

In Section III we apply this formalism to the case in which a cylindrical waveguide is present. We show that if the interaction is strong enough and the difference between the phase velocities of neighboring vacuum waveguide modes is small enough, the actual eigenmodes of the FEL system significantly differ from the vacuum

Manuscript received September 23, 1989; revised December 11, 1989. This work was supported by the Koret Foundation.

The author is with the Department of Physics, The Weizmann Institute of Science, Rehovot 76100, Israel.

IEEE Log Number 9035366.

waveguide modes. Each FEL eigenmode is a superposition of several vacuum waveguide modes. This coupling of several vacuum waveguide modes has been experimentally demonstrated and theoretically analyzed by the Columbia group [11], [23]. In their experiment the amplified wave was allowed to propagate beyond the point at which the electron beam had been terminated. An interference pattern was exhibited between the several vacuum waveguide modes of which the FEL eigenmode was composed. As mentioned above, our analysis confirms their results. In addition, we are also able to analytically derive expressions for the wavefield profile and a dispersion relation.

In Section IV we present an energy integral which determines the domain in the complex plane where nonreal eigenvalues are allowed. This domain is circular when the electron beam has a uniform density, and has the shape of a stadium when the density is not uniform.

In Section V we apply our formalism to the FEL interaction in the Raman regime when no waveguide or cavity is present. We look for eigenmodes that vanish at an infinite radial distance. Following Moore's analysis for the strong-pump regime [3], we identify a coupling parameter for the Raman regime. When the coupling parameter is large the growing waves are confined to the beam volume. The effective filling factor is then one and the gain scales as in the one-dimensional case. The opposite happens in the case of a small coupling parameter. The growing modes still have a transverse profile which vanishes at a distance from the beam axis. The transverse cross section of the wave, however, is much larger than that of the electron beam, corresponding to a small filling factor. The gain is reduced relative to the one-dimensional scaling because of these diffraction losses. The particular scaling of the gain when diffraction is large depends on the FEL regime of operation, and is different in the collective Raman regime from the scaling in the strong-pump Compton regime. The diffraction losses depend also on the geometry. In previous papers we studied the FEL interaction of a sheet electron beam in the strong-pump regime [16] and Raman regime [27]. The coupling parameter and scaling of the gain when this coupling parameter was small were different from those of the FEL interaction of a cylindrical electron beam. A comparison between the different scalings of the gain of sheet-beam and cylindrical-beam FEL's in the Compton and Raman regimes is presented in [27]. In each of these four cases, varying the beam transverse dimensions, while keeping the beam current fixed, has two opposing effects. When the beam transverse dimensions are reduced the density increases and the gain grows. On the other hand, the decrease in beam dimensions causes the coupling parameter to be reduced and the effective filling factor to decrease, and this has the opposite effect of reducing the gain. We show that in our case, the presence of these two effects results in a nonmonotonic dependence of the gain on the beam radius. In a different regime of operation or in a different geometry, the behavior of the gain, when the beam transverse dimension is reduced, may be different.

In Section VI we study numerically the influence of the waveguide radius (as opposed to the beam radius of Section V) on the wave growth rate and wave profile in the FEL.

II. The General Formalism

The electron-beam dynamics is governed by the cold-fluid equations. These are the continuity equation:

$$\frac{1}{c}\frac{\partial}{\partial t}(H\gamma) + \underline{\nabla}\cdot(H\underline{P}) = 0 \tag{1}$$

and the momentum equation:

$$\frac{\gamma}{c}\frac{\partial \underline{P}}{\partial t} + \underline{P}\cdot\underline{\nabla}\underline{P} = -(\gamma\underline{E} + \underline{P}\times\underline{B}). \tag{2}$$

Here $\underline{P} \equiv \gamma\underline{v}/c$ is the normalized momentum, c is the velocity of light in vacuum, $\underline{v}$ is the electron velocity, and γ is

$$\gamma^2 = 1 + \underline{P}\cdot\underline{P}. \tag{3}$$

Also, H is the normalize fluid density,

$$H \equiv \omega_p^2/(c^2\gamma) \tag{4}$$

where ω_p is the plasma frequency. The fields $\underline{E}$ and $\underline{B}$ are the electric and magnetic fields multiplied by (e/mc^2), where $-e$ and m are the electron charge and mass.

The electron beam is assumed to propagate along a helical magnetic wiggler of the approximate form:

$$\underline{B}_w = B_w(\hat{e}_r\cos\varphi - \hat{e}_\theta\sin\varphi). \tag{5}$$

Here φ is the helical coordinate,

$$\varphi \equiv \theta - k_w z \tag{6}$$

where r, θ, and z are the usual cylindrical coordinates. We assume that the beam is thin:

$$k_w r_b \ll 1 \tag{7}$$

(r_b is the beam radius) so that we may approximate the wiggler field by its form on-axis. The equilibrium flow is assumed to be helical:

$$\underline{P} = \underline{p} = -\frac{B_w}{k_w}(\hat{e}_r\cos\varphi - \hat{e}_\theta\sin\varphi) + [\gamma^2 - 1 - a_w^2]^{1/2}\hat{e}_z \tag{8}$$

where $a_w \equiv B_w/k_w$. We assume that the transverse excursion of the electrons is much smaller than the beam radius r_b so that the beam envelope is not distorted by the electron wiggling and preserves its cylindrical shape.

We now turn to the linearized equations. We assume that

$$p_\perp \ll p_z \tag{9}$$

and that the perturbed quantities vary mainly axially and not transversely:

$$\frac{\partial\delta g}{\partial r}, \frac{\partial\delta g}{\partial\theta} \ll \frac{\partial\delta g}{\partial z}. \tag{10}$$

The requirement of a small transverse excursion, together with (7) and (9), are combined to $a_w/(\gamma^2 - 1 - a_w^2)^{1/2} << k_w r_b << 1$. Using the two assumptions (9) and (10), we neglect terms of the type $p_r(\partial/\partial r)$ and $p_\theta(\partial/\partial\theta)$ in the cold-fluid equations. We write each quantity as

$$G(r, \varphi, z, t) = g(r, \varphi) + \mathrm{Re}\left[\sum_{n=-\infty}^{\infty} \delta g^{(n)}(r) e^{in\varphi + iqz - i\omega t}\right]. \quad (11)$$

We limit ourselves to the case in which one helical harmonic is dominant; say $n = l$. Then noting that

$$\frac{\partial}{\partial z} = \frac{\partial}{\partial z} - k_w \frac{\partial}{\partial \varphi} \quad (12a)$$

and that

$$\frac{\partial}{\partial \theta} = \frac{\partial}{\partial \varphi} \quad (12b)$$

we define

$$k_z \equiv q - lk_w. \quad (12c)$$

In this case $\delta\underline{E}_\perp^{(l)}$ and $\delta\underline{B}_\perp^{(l)}$ are dominant and are coupled to $\delta h^{(l-1)}$ and $\delta\underline{E}_z^{(l-1)}$, the slow-wave components. The continuity equation for $\delta h^{(l-1)}$ becomes

$$\left[-\gamma\omega/c + (k_z + k_w)p_z\right]\delta h^{(l-1)} = h\left[p_z\omega/(\gamma c) - (k_z + k_w)\right]\delta p_z^{(l-1)}. \quad (13)$$

Here we used the approximate relation,

$$\gamma\delta\gamma^{(l-1)} = p_z\delta p_z^{(l-1)}. \quad (14)$$

We assume that $\delta h^{(l-1)}$ becomes large and that k_z is such that

$$\left|k_z + k_w - \gamma\omega/p_z c\right| << k_w. \quad (15)$$

The momentum equation for $\delta p_z^{(l-1)}$ becomes

$$i\left[-\gamma\omega/c + (k_z + k_w)p_z\right]\delta p_z^{(l-1)} = -\gamma\delta E_z^{(l-1)} + \frac{ck_z}{\omega} a_w \delta E_+^{(l)} \quad (16)$$

where

$$\delta E_\pm \equiv \frac{(\delta E_r \mp i\delta E_\theta)}{2}. \quad (17)$$

We express the normalized charge density ρ (the charge density multiplied by 4π) and normalized current density $\underline{j}$ (the current density multiplied by $4\pi/c$) as

$$\rho = -H\gamma \quad (18)$$

and

$$\underline{j} = -H\underline{P}. \quad (19)$$

Gauss' law for $\delta E_z^{(l-1)}$ is

$$i(k_z + k_w)\delta E_z^{(l-1)} = -\gamma\delta h^{(l-1)} - \frac{hp_z}{\gamma}\delta p_z^{(l-1)} \quad (20)$$

for which we used again (14). Note that the transverse dependence of this slow wave is omitted. It is assumed that the FEL interaction determines the transverse dependence of $\delta E_z^{(l-1)}$. The question of the transverse dependence of this slow space-charge wave was recently addressed by Jerby and Gover [20].

Equations (13), (14), and (20) are algebraic equations for $\delta h^{(l-1)}$, $\delta p_z^{(l-1)}$, and $\delta E_z^{(l-1)}$. They have the same form as they have in the one-dimensional analysis as a result of assumption (10). The perturbed density becomes:

$$\delta h^{(l-1)} = \frac{iha_w(k_z + k_w - p_z\omega/\gamma c)\delta E_+^{(l)}}{\left\{\left[(k_z + k_w)p_z - \gamma\omega/c\right]^2 - h(1 + a_w^2)\right\}}. \quad (21)$$

The lth harmonic of the perturbed perpendicular current, to lowest order, is

$$\delta j_r^{(l)} = \frac{a_w}{2}\delta h^{(l-1)} \quad (22)$$

$$\delta j_\theta^{(l)} = \frac{ia_w}{2}\delta h^{(l-1)}. \quad (23)$$

Using (21)–(23), we now write the transverse currents as

$$\delta j_\theta^{(l)} = i\delta j_r^{(l)} = -Q\delta E_+^{(l)} \quad (24)$$

where

$$Q \equiv \frac{ha_w^2(k_z + k_w - p_z\omega/\gamma c)}{2\left\{\left[(k_z + k_w)p_z - \gamma\omega/c\right]^2 - h(1 + a_w^2)\right\}}. \quad (25)$$

The expressions for $\delta j_\perp^{(l)}$ are similar to those in the one-dimensional analysis. The transverse dependence, however, makes $\delta\rho^{(l)}$ and $\delta j_z^{(l)}$ also large. In order to show that $\delta\rho^{(l)}$ and $\delta j_z^{(l)}$ are large, we write the lth helical harmonic of the continuity equation:

$$i(k_z p_z - \gamma\omega/c)\delta h^{(l)} = -ih(k_z - \omega p_z/c\gamma)\delta p_z^{(l)} + \frac{a_w}{2}\left[\frac{\partial}{\partial r} - \frac{(l-1)}{r}\right]\delta h^{(l-1)} \quad (26)$$

and the lth helical harmonic of the longitudinal component of the momentum equation:

$$i(k_z p_z - \gamma\omega/c)\delta p_z^{(l)} = -\gamma\delta E_z^{(l)} + \frac{a_w}{2}\left[\frac{\partial}{\partial r} - \frac{(l-1)}{r}\right]\delta p_z^{(l-1)}. \quad (27)$$

We used the approximate relation $\gamma\delta\gamma^{(l)} = p_z\delta p_z^{(l)}$. From these equations it is clear that the large perturbed density $\delta h^{(l-1)}$ and momentum $\delta p_z^{(l-1)}$ contribute to $\delta h^{(l)}$ and $\delta p_z^{(l)}$ and therefore to $\delta\rho^{(l)}$ and $\delta j_z^{(l)}$ through the transverse dependence. We use the expressions:

$$\delta\rho^{(l)} = -(hp_z/\gamma)\delta p_z^{(l)} - \gamma\delta h^{(l)} \quad (28)$$

and

$$\delta j_z^{(l)} = -h\delta p_z^{(l)} - p_z\delta h^{(l)} \quad (29)$$

and write the perturbed density and current as

$$\delta\rho^{(l)} = \frac{ihk_z(1 + a_w^2)\delta E_z^{(l)}}{(k_z p_z - \gamma\omega/c)^2} + \frac{ia_w}{2(k_z p_z - \gamma\omega/c)} \cdot \left[\frac{\partial}{\partial r} - \frac{(l-1)}{r}\right] \left[-\frac{hk_z(1 + a_w^2)\delta p_z^{(l-1)}}{\gamma(k_z p_z - \gamma\omega/c)} + \gamma\delta h^{(l-1)}\right] \quad (30)$$

and

$$\delta j_z^{(l)} = \frac{ih\omega(1 + a_w^2)\delta E_z^{(l)}}{c(k_z p_z - \gamma\omega/c)^2} + \frac{ia_w}{2(k_z p_z - \gamma\omega/c)} \cdot \left[\frac{\partial}{\partial r} - \frac{(l-1)}{r}\right] \left[-\frac{h\omega(1 + a_w^2)\delta p_z^{(l-1)}}{c\gamma(k_z p_z - \gamma\omega/c)} + p_z\delta h^{(l-1)}\right]. \quad (31)$$

Note that $\delta\rho^{(l)}$, $\delta j_r^{(l)}$, $\delta j_\theta^{(l)}$, and $\delta j_z^{(l)}$, as expressed in (22)–(24), (30), and (31), satisfy the continuity equation. Using assumption (15) in expressions (30) and (31), we find that the contribution of $\delta h^{(l-1)}$ is larger than the contribution of $\delta p_z^{(l-1)}$. We make the further assumption that the second terms in the expressions (30) and (31) are larger than the first terms. Thus $\delta\rho^{(l)}$ and $\delta j_z^{(l)}$ are determined mainly by the resonant $\delta h^{(l-1)}$. We therefore approximate:

$$\delta\rho^{(l)} = -\frac{\gamma}{(k_z p_z - \gamma\omega/c)}\left[\frac{\partial}{\partial r} - \frac{(l-1)}{r}\right](Q\delta E_+^{(l)}) \quad (32)$$

$$\delta j_z^{(l)} = -\frac{p_z}{(k_z p_z - \gamma\omega/c)}\left[\frac{\partial}{\partial r} - \frac{(l-1)}{r}\right](Q\delta E_+^{(l)}). \quad (33)$$

We have completed the derivation of the expressions for the charge and current densities and now turn to the wave fields.

The evolution of the wave fields is governed by the Maxwell equations,

$$\nabla^2\underline{B} - \frac{1}{c^2}\frac{\partial^2\underline{B}}{\partial t^2} = -\underline{\nabla}\times\underline{j} \quad (34)$$

$$\nabla^2\underline{E} - \frac{1}{c^2}\frac{\partial^2\underline{E}}{\partial t^2} = \underline{\nabla}\rho + \frac{1}{c}\frac{\partial\underline{j}}{\partial t}. \quad (35)$$

The transverse components of (35) yield the two coupled equations,

$$\left(\nabla^2 \pm \frac{(2l \mp 1)}{r^2} + \frac{\omega^2}{c^2}\right)\delta E_\pm^{(l)} = \frac{1}{2}\left(\frac{\partial}{\partial r} \pm \frac{l}{r}\right)\delta\rho^{(l)} - \frac{i\omega}{c}\delta j_\pm^{(l)} \quad (36)$$

where $\delta j_\pm \equiv \frac{1}{2}(\delta j_r \mp i\delta j_\theta)$. Examining the expressions for $\delta\rho^{(l)}$ and $\delta\underline{j}^{(l)}$ and assuming the transverse dependence of the fields to be weaker than the z dependence, we neglect the first term on the right-hand side (RHS) of the equation. Also, following (24),

$$\delta j_+^{(l)} = iQ\delta E_+^{(l)} \quad (37)$$

$$\delta j_-^{(l)} = 0. \quad (38)$$

One pair of governing equations is, therefore,

$$\frac{1}{r}\frac{\partial}{\partial r}\left(r\frac{\partial\delta E_+^{(l)}}{\partial r}\right) + \left[\frac{\omega^2}{c^2} - k_z^2 - \frac{(l-1)^2}{r^2} - \frac{\omega}{c}Q\right] \cdot \delta E_+^{(l)} = 0 \quad (39)$$

$$\frac{1}{r}\frac{\partial}{\partial r}\left(r\frac{\partial\delta E_-^{(l)}}{\partial r}\right) + \left[\frac{\omega^2}{c^2} - k_z^2 - \frac{(l+1)^2}{r^2}\right]\delta E_-^{(l)} = 0 \quad (40)$$

where Q is defined in (25). The equation for $\delta E_-^{(l)}$ is the same as in vacuum. The FEL interaction is expressed through the presence of the term Q in the equation for $\delta E_+^{(l)}$. If there is no transverse dependence and therefore $l = 1$, (39) is reduced to the one-dimensional dispersion relation,

$$\frac{\omega^2}{c^2} - k_z^2 - \frac{\omega}{c}Q = 0. \quad (41)$$

We now derive an equivalent form of the governing equations (39) and (40). When the FEL interaction in a waveguide is considered, it is sometimes convenient to write the equations for δE_z and δB_z. The z components of (34) and (35) are

$$\left(\nabla^2 + \frac{\omega^2}{c^2}\right)\delta B_z^{(l)} = -\frac{4\pi}{c}\left[\frac{1}{r}\frac{\partial}{\partial r}(r\delta j_\theta^{(l)}) - \frac{il}{r}\delta j_r^{(l)}\right] = \left[\frac{\partial}{\partial r} - \frac{(l-1)}{r}\right](Q\delta E_+^{(l)}) \quad (42)$$

$$\left(\nabla^2 + \frac{\omega^2}{c^2}\right)\delta E_z^{(l)} = ik_z 4\pi\delta\rho^{(l)} - \frac{4\pi i\omega}{c^2}\delta j_z^{(l)} = -\frac{i(k_z\gamma - p_z\omega/c)}{(k_z p_z - \gamma\omega/c)}\left[\frac{\partial}{\partial r} - \frac{(l-1)}{r}\right] \cdot (Q\delta E_+^{(l)}) \quad (43)$$

where we used (24), (32), and (33) for $\delta\underline{j}^{(l)}$ and $\delta\rho^{(l)}$. From Maxwell's equation it is easy to derive the following relations:

$$\left(\frac{\partial}{\partial r} + \frac{l}{r}\right)\left(\frac{\omega}{c}\delta B_z^{(l)} - ik_z\delta E_z^{(l)}\right) = -2\left(\frac{\omega^2}{c^2} - k_z^2\right)\delta E_+^{(l)} - \frac{2i\omega}{c}\delta j_+^{(l)} \quad (44)$$

and

$$\left(\frac{\partial}{\partial r} - \frac{l}{r}\right)\left(\frac{\omega}{c}\,\delta B_z + ik_z\delta E_z\right) = 2\left(\frac{\omega^2}{c^2} - k_z^2\right)\delta E_-^{(l)} + \frac{2i\omega}{c}\,\delta j_-^{(l)}. \tag{45}$$

Upon using the expressions for the currents, these two last equations become

$$\left(\frac{\partial}{\partial r} + \frac{l}{r}\right)\left(\frac{\omega}{c}\,\delta B_z^{(l)} - ik_z\delta E_z^{(l)}\right) = -2\left(\frac{\omega^2}{c^2} - k_z^2 - \frac{\omega}{c}\,Q\right)\delta E_+^{(l)} \tag{46}$$

and

$$\left(\frac{\partial}{\partial r} - \frac{l}{r}\right)\left(\frac{\omega}{c}\,\delta B_z^{(l)} + ik_z\delta E_z^{(l)}\right) = 2\left(\frac{\omega^2}{c^2} - k_z^2\right)\delta E_-^{(l)}. \tag{47}$$

After some algebraic manipulation we obtain from (42), (43), (46), and (47) two decoupled equations,

$$\left(\frac{\partial^2}{\partial r^2} + \frac{1}{r}\frac{\partial}{\partial r} - \frac{l^2}{r^2} + \frac{\omega^2}{c^2} - k_z^2\right)\left(\delta B_z^{(l)} - \frac{i}{U}\,\delta E_z^{(l)}\right) = 0 \tag{48}$$

$$\left[\frac{\partial^2}{\partial r^2} + \frac{1}{r}\frac{\partial}{\partial r} - \frac{l^2}{r^2} + \left(\frac{\omega^2}{c^2} - k_z^2 - \frac{\omega}{c}\,Q\right)G\right] \cdot \left(\frac{\omega}{c}\,\delta B_z^{(l)} - ik_z\delta E_z^{(l)}\right) = 0. \tag{49}$$

Here,

$$U \equiv (k_z\gamma - p_z\omega/c)/(k_z p_z - \gamma\omega/c) \tag{50a}$$

and

$$G \equiv 2\left(\frac{\omega^2}{c^2} - k_z^2\right)\Big/\left[2\left(\frac{\omega^2}{c^2} - k_z^2\right) - Q\left(\frac{\omega}{c} + k_z U\right)\right]. \tag{50b}$$

By operating on (46) and (47) with $[(\partial/\partial r) - ((l-1)/r)]$ and $[(\partial/\partial r) + ((l-1)/r)]$, respectively, and by using (48) and (49) we derive the following relations:

$$G\left(\frac{\omega}{c}\,\delta B_z^{(l)} - ik_z\delta E_z^{(l)}\right) = 2\left[\frac{\partial}{\partial r} - \frac{(l-1)}{r}\right]\delta E_+^{(l)} \tag{51}$$

and

$$2\left(\frac{\omega^2}{c^2} - k_z^2\right)k_z\frac{\omega}{c}\left(\delta B_z^{(l)} - \frac{i}{U}\,\delta E_z^{(l)}\right) - G\left(\frac{\omega}{Uc} + k_z\right)\left(\frac{\omega^2}{c^2} - k_z^2 - \frac{\omega}{c}\,Q\right)\left(\frac{\omega}{c}\,\delta B_z^{(l)} - ik_z\delta E_z^{(l)}\right) = -2(k_z - \omega/Uc)\left(\frac{\omega^2}{c^2} - k_z^2\right)\left[\frac{\partial}{\partial r} + \frac{(l+1)}{r}\right]\delta E_-^{(l)}. \tag{52}$$

Equations (39), (40), (48), and (49) are equations for $\delta E_+^{(l)}$, $\delta E_-^{(l)}$, $(\delta B_z^{(l)} - i/U\delta E_z^{(l)})$, and $((\omega/c)\delta B_z^{(l)} - ik_z\delta E_z^{(l)})$, with the unknown parameter (eigenvalue) k_z. Even though these equations are not coupled, the boundary conditions usually couple the unknowns.

We can solve equations (48) and (49) for $\delta B_z^{(l)}$ and $\delta E_z^{(l)}$ and for the eigenvalue k_z and then find $\delta E_r^{(l)}$ and $\delta E_\theta^{(l)}$ from equations (46) and (47). Alternatively, we can solve equations (39) and (40) for the transverse fields $\delta E_r^{(l)}$ and $\delta E_\theta^{(l)}$ and then use (51) and (52) to find the longitudinal fields $\delta E_z^{(l)}$ and $\delta B_z^{(l)}$.

The expressions for U and G are simplified if we use inequality (15) and assume $k_z \cong \omega/c$. Then,

$$\omega/c \cong k_w\gamma(\gamma + p_z)/(1 + a_w^2) \tag{53}$$

as in the one-dimensional case. We may then approximate $U \cong -\gamma^2/p_z^2$. For a relativistic beam $\gamma \cong p_z$, $U \cong -1$ and $G \cong 1$. We then also approximate:

$$Q \cong \frac{hk_w a_w^2}{\left\{\left[(k_z + k_w)p_z - \gamma\omega/c\right]^2 - h(1 + a_w^2)\right\}} = \frac{\omega_p^2 k_w a_w^2}{\left\{\left[k_z + k_w - \omega/v_z\right]^2 - (\omega_p^2/\gamma^3 v_z^2)(1 + a_w^2)\right\}}. \tag{54}$$

We will employ these approximations in the following. Equations (48) and (49) are simplified to

$$\left(\frac{\partial^2}{\partial r^2} + \frac{1}{2}\frac{\partial}{\partial r} - \frac{l^2}{r^2} + \frac{\omega^2}{c^2} - k_z^2\right)(\delta B_z^{(l)} + i\delta E_z^{(l)}) = 0 \tag{55}$$

$$\left(\frac{\partial^2}{\partial r^2} + \frac{1}{r}\frac{\partial}{\partial r} - \frac{l^2}{r^2} + \frac{\omega^2}{c^2} - k_z^2 - \frac{\omega}{c}\,Q\right) \cdot (\delta B_z^{(l)} - i\delta E_z^{(l)}) = 0. \tag{56}$$

Relations (46) and (47) become:

$$\frac{\omega}{c}\left(\frac{\partial}{\partial r} + \frac{l}{r}\right)(\delta B_z^{(l)} - i\delta E_z^{(l)}) = -2\left(\frac{\omega^2}{c^2} - k_z^2 - \frac{\omega}{c}\,Q\right)\delta E_+^{(l)} \tag{57}$$

and

$$\frac{\omega}{c}\left(\frac{\partial}{\partial r} - \frac{l}{r}\right)(\delta B_z^{(l)} + i\delta E_z^{(l)}) = 2\left(\frac{\omega^2}{c^2} - k_z^2\right)\delta E_-^{(l)}. \tag{58}$$

Also, (51) and (52) become:

$$\frac{\omega}{c}\left(\delta B_z^{(l)} - i\delta E_z^{(l)}\right) = 2\left[\frac{\partial}{\partial r} - \frac{(l-1)}{r}\right]\delta E_+^{(l)} \quad (59)$$

and

$$\frac{\omega}{c}\left(\delta B_z^{(l)} + i\delta E_z^{(l)}\right) = 2\left[\frac{\partial}{\partial r} + \frac{(l+1)}{r}\right]\delta E_-^{(l)}. \quad (60)$$

From (57)–(60) we see that if $\delta E_+^{(l)}$ and $\delta E_-^{(l)}$ and their derivatives are continuous, the fields $\delta E_z^{(l)}$ and $\delta B_z^{(l)}$ are continuous as well. However, the derivatives of $\delta E_z^{(l)}$ and $\delta B_z^{(l)}$ have a discontinuity at $r = r_b$ if Q is not continuous there (because the density is not continuous). Had we not employed the approximations $k_z \cong \omega/c$ and $p_z \cong \gamma$, the fields $\delta E_z^{(l)}$ and $\delta B_z^{(l)}$ would have a discontinuity as well. The jump at $r = r_b$ in the derivatives of $\delta B_z^{(l)}$ and $\delta E_z^{(l)}$ is found from (57) and (58). From (58) we find that

$$\left[\frac{\partial}{\partial r}\left(\delta B_z^{(l)} + i\delta E_z^{(l)}\right)\right]_{r=r_b} = 0 \quad (61)$$

while from (57) and (58) we find that

$$\left[\frac{\partial \delta B_z^{(l)}}{\partial r}(r = r_b^+) - \frac{\partial \delta B_z^{(l)}}{\partial r}(r = r_b^-)\right]$$

$$= -Q(r = r_b^-)\delta E_+^{(l)}(r_b) = -\frac{\omega}{c}Q(r = r_b^-)$$

$$\cdot\left[\left(\frac{\partial}{\partial r} + \frac{l}{r}\right)\left(\delta B_z^{(l)} - i\delta E_z^{(l)}\right)\right.$$

$$\left.\cdot\left(\frac{\omega^2}{c^2} - k_z^2 - \frac{\omega}{c}Q\right)^{-1}\right](r = r_b^-). \quad (62)$$

The boundary condition at the origin is regularity.

The assumption of a cylindrical cross-section beam involves a neglect of the beam-wiggling motion, which can be modeled by surface charge and current distributions. These surface charge and current could have a significant effect when the beam radius is small.

We have completed the derivation of the governing equations and of the boundary conditions at $r = 0$ and $r = r_b$. In the next sections we study two cases. First, the case of a cylindrical waveguide, and secondly, the case when such a waveguide is not present.

III. The Case of a Cylindrical Waveguide

Let us assume that a perfectly conducting wall is located at $r = R$. The boundary conditions there are $\delta E_z = 0$ and $(\partial \delta B_z/\partial r) = 0$ or $\delta E_\theta = 0$ and $(\partial/\partial r)(r\delta E_r) = 0$.

The equilibrium beam density is assumed here to be constant:

$$h = \text{const}, \qquad r \le r_b$$

$$h = 0, \qquad r > r_b. \quad (63)$$

The solutions of (39) and (40) are

$$\delta E_- = A_1 J_{l+1}(k_\perp r), \qquad 0 \le r \le R \quad (64a)$$

and

$$\delta E_+ = A_2 J_{l-1}(Sr), \qquad 0 \le r \le r_b \quad (64b)$$

$$\delta E_+ = A_3 J_{l-1}(k_\perp r) + A_4 Y_{l-1}(k_\perp r), \qquad r_b \le r \le R \quad (64c)$$

where

$$k_\perp^2 \equiv \omega^2 - k_z^2 \quad (65a)$$

and

$$S^2 \equiv \omega^2 - k_z^2 - \frac{\omega}{c}Q. \quad (65b)$$

The quantities Q and S are constant because h is constant for $r \le r_b$. Note again that $S = 0$ is the one-dimensional dispersion relation. From the continuity of the fields and their derivatives at $r = r_b$ we obtain:

$$A_2 J_{l-1}(Sr_b) = A_3 J_{l-1}(k_\perp r_b) + A_4 Y_{l-1}(k_\perp r_b) \quad (66a)$$

$$\frac{S}{k_\perp} A_2 J_{l-1}(Sr_b) = A_3 J_{l-1}(k_\perp r_b) + A_4 Y_{l-1}(k_\perp r_b). \quad (66b)$$

The requirements $\delta E_\theta = 0$ and $(\partial/\partial r)(r\delta E_r) = 0$ at $r = R$ yield:

$$A_1 J_{l+1}(k_\perp R) = A_3 J_{l-1}(k_\perp R) + A_4 Y_{l-1}(k_\perp R) \quad (67a)$$

$$A_1 \frac{\partial}{\partial r}\left[rJ_{l-1}(k_\perp r)\right]\Big|_{r=R} + A_3 \frac{\partial}{\partial r}\left[rJ_{l-1}(k_\perp r)\right]\Big|_{r=R}$$

$$+ A_4 \frac{\partial}{\partial r}\left[rY_{l-1}(k_\perp r)\right]\Big|_{r=R} = 0. \quad (67b)$$

The solvability condition of these equations yields the dispersion relation. First, from (67a) and (67b) we find that

$$\frac{A_3}{A_1} = \pi k_\perp R J_l(k_\perp R) Y_l'(k_\perp R) - 1 \quad (68a)$$

and

$$\frac{A_4}{A_1} = -\pi k_\perp R J_l(k_\perp R) J_l'(k_\perp R). \quad (68b)$$

We then use these expressions in (66a) and (66b) and obtain the dispersion relation:

$$\left[\pi k_\perp R J_l(k_\perp R) Y_l'(k_\perp R) - 1\right]$$

$$\cdot\left[SJ_{l-1}'(Sr_b) J_{l-1}(k_\perp r_b) - k_\perp J_{l-1}'(k_\perp r_b) J_{l-1}(Sr_b)\right]$$

$$- \pi k_\perp R J_l(k_\perp R) J_l'(k_\perp R)\left[SJ_{l-1}'(Sr_b) Y_{l-1}(k_\perp r_b)\right.$$

$$\left. - k_\perp Y_{l-1}'(k_\perp r_b) J_{l-1}(Sr_b)\right] = 0. \quad (69)$$

Both $k_\perp$ and S are functions of the eigenvalue k_z. After numerically finding k_z, one can calculate A_3 and A_4

through (68a) and (68b), and A_2 through (66a) or (66b). For completeness, we use (59) and (60) as well and write the explicit expressions for all the field components ($r \le r_b$):

$$\delta E_r = A_1 J_{l+1}(k_\perp r) + A_2 J_{l-1}(Sr)$$
$$\delta E_\theta = -i\left[A_1 J_{l+1}(k_\perp r) - A_2 J_{l-1}(Sr)\right]$$
$$\delta E_z = -\frac{ic}{\omega}\left[A_1 k_\perp J_l(k_\perp r) + A_2 S J_l(Sr)\right]$$
$$\delta B_z = \frac{c}{\omega}\left[A_1 k_\perp J_l(k_\perp r) - A_2 S J_l(Sr)\right]. \quad (70)$$

When $R \ge r \ge r_b$ the wave fields are

$$\delta E_r = A_1 J_{l+1}(k_\perp r) + A_3 J_{l-1}(k_\perp r) + A_4 Y_{l-1}(k_\perp r)$$
$$\delta E_\theta = -i\left[A_1 J_{l+1}(k_\perp r) - A_3 J_{l-1}(k_\perp r) - A_4 Y_{l-1}(k_\perp r)\right]$$
$$\delta E_z = -i\frac{k_\perp c}{\omega}\left[(A_3 + A_1) J_l(k_\perp r) + A_4 Y_l(k_\perp r)\right]$$
$$\delta B_z = -\frac{k_\perp c}{\omega}\left[(A_3 - A_1) J_l(k_\perp r) + A_4 Y_l(k_\perp r)\right]. \quad (71)$$

Similarly, expressions for δB_r and δB_θ could be derived.

The effects of the waveguide and FEL interaction on the wave transverse profile are clearly seen by examining (55) and (56). In vacuum, when no beam is present, $Q = 0$ and the two equations are identical. The equations for δB_z and δE_z can be decoupled, and there are independent solutions that correspond to TE and TM modes. On the other hand, if the FEL employs a cylindrical beam with no waveguide, the equations for $\delta B_z + i\delta E_z$ and $\delta B_z - i\delta E_z$ could be decoupled. The noninteracting part $\delta B_z + i\delta E_z$ is zero and one can solve for $\delta B_z - i\delta E_z$ (or equivalently for δE_+). The presence of the waveguide prevents $\delta B_z + i\delta E_z$ from being identically zero because of the boundary conditions at the wall. The FEL interaction in the presence of a waveguide supports, therefore, waves that are neither TE nor TM waves. These waves are also not purely right-hand polarized and are composed of both $\delta B_z - i\delta E_z$ and $\delta B_z + i\delta E_z$ (δE_+ and δE_-). Recent work by Hartemann *et al.* [30] also uses an eigenvalue formalism to study an FEL in a cylindrical waveguide. Their work analyzes the effects of a guide magnetic field in more detail, but they seem to use a more approximated form by neglecting the coupling of the TE and TM modes and retaining the TE modes only. Some of their results are similar to those of the present work.

IV. An Energy Integral in the Case of Nonuniform Beam Density

In this section we study an FEL which employs an electron beam of nonuniform density that varies radially. We assume that the density nonuniformity is small and write:

$$\omega_p^2(r) = \omega_{po}^2 + \omega_{p1}^2(r) \quad (72a)$$

and

$$h(r) = h_0 + h_1(r) \quad (72b)$$

where

$$\left|\omega_{p1}^2(r)\right| \ll \omega_{p0}^2 \quad (73a)$$

and

$$\left|h_1(r)\right| \ll h_0. \quad (73b)$$

We define a new eigenvalue,

$$\nu \equiv k_z + k_w - \omega/v_z - (\omega_{po}/v_z\gamma^{3/2})(1 + a_w^2)^{1/2} \quad (74)$$

and assume:

$$|\nu| \ll (\omega_{po}/v_z\gamma^{3/2})(1 + a_w^2)^{1/2}. \quad (75)$$

We may now approximate:

$$Q = \frac{\beta}{[\nu - f(r)]} \quad (76)$$

where

$$\beta \equiv \frac{\omega_{po} k_w a_w^2}{2\gamma^{3/2} v_z (1 + a_w^2)^{1/2}} \quad (77)$$

and

$$f(r) \equiv \frac{\omega_{p1}(r)}{v_z\gamma^{3/2}}(1 + a_w^2)^{1/2}. \quad (78)$$

We also write

$$\frac{\omega^2}{c^2} - k_z^2 = (\nu - \xi)\left(\frac{\omega}{c} + k_z\right) \quad (79)$$

where ξ, the detuning parameter, is

$$\xi = k_w - \frac{\omega}{c}\left(\frac{c}{v_z} - 1\right) - \frac{\omega_{p0}}{v_z\omega^{3/2}}\left(1 + a_w^2\right)^{1/2}. \quad (80)$$

In the one-dimensional case $\xi = 0$ corresponds to the FEL resonance. We assume that the transverse dependence is larger than the longitudinal dependence and that therefore ξ is much smaller than ω/c. We also approximate $(\omega/c) + k_z = 2(\omega/c)$.

With these definitions we write (39) and (40) in the following forms:

$$\frac{\partial}{\partial r}\left[\frac{1}{r}\frac{\partial}{\partial r}(r\delta E_+)\right] + \left[-2\frac{\omega}{c}(\nu - \xi) - \frac{l(l-2)}{r^2} - \frac{\omega}{c}Q\right]\delta E_+ = 0 \quad (81)$$

$$\frac{\partial}{\partial r}\left[\frac{1}{r}\frac{\partial}{\partial r}(r\delta E_-)\right] + \left[-2\frac{\omega}{c}(\nu - \xi) - \frac{l(l+2)}{r^2}\right]\delta E_- = 0. \quad (82)$$

We multiply (81) by $r\delta E_+^*$ and (22) by $r\delta E_-^*$, integrate on r from zero to R, and add the two equations. Using integration by parts, the regularity of the solutions at $r = 0$, and the boundary conditions at the wall, we find, similarly to [10] and [16], that

$$2\left(|\delta E_r|_{r=0}^2 + |\delta E_\theta|_{r=0}^2\right) - \int_0^R \frac{dr}{r}\left(\left|\frac{\partial}{\partial r}(r\delta E_+)\right|^2 + \left|\frac{\partial}{\partial r}(r\delta E_-)\right|^2\right) + \int_0^R drr\left(-2\frac{\omega}{c}(\nu - \xi) - \frac{l^2}{r^2}\right)\left(|\delta E_+|^2 + |\delta E_-|^2\right) + \int_0^R dr\frac{2l}{r}\left(|\delta E_+|^2 - |\delta E_-|^2\right) - \frac{\omega}{c}\int_0^R drrQ|\delta E_+|^2 = 0. \tag{83}$$

Taking the imaginary part of this equality, we obtain:

$$\int_0^R drr\nu_i\left\{2\left(|\delta E_+|^2 + |\delta E_-|^2\right) - \frac{\beta|\delta E_+|^2}{|\nu - f(r)|^2}\right\} = 0. \tag{84}$$

We look for nonreal eigenvalues for which $\nu_i \neq 0$. The term in the curly brackets has to take both positive and negative values. Therefore, there must be $r_0 \epsilon [0, R]$ such that

$$\frac{\beta|\delta E_+|^2}{|\nu - f(r_0)|^2} > 2\left(|\delta E_+|^2 + |\delta E_-|^2\right) \tag{85}$$

or

$$\frac{\beta}{|\nu - f(r_0)|^2} > 2. \tag{86}$$

This last inequality determines a domain in the complex ν plane where nonreal eigenvalues are allowed. Assume that the range of f is

$$f_{\min} \leq f(r) \leq f_{\max}, \qquad |r| < R. \tag{87}$$

The domain of allowed eigenvalues is shown in Fig. 1. It has the form of a stadium; a rectangle and two half-circles of radius $(\beta/2)^{1/2}$. When the density of the beam is uniform, the stadium shrinks into a circle. The case in which

$$|f_{\max} - f_{\min}| \gg (\beta/2)^{1/2} \tag{88}$$

was analyzed by Fruchtman and Weitzner for a sheet beam [18]. It can be analyzed in a similar way for a cylindrical geometry.

In the next section we return to the case of a uniform density beam. We derive asymptotic expressions for the gain when optical guiding is strong and when diffraction is large.

V. Asymptotic Expressions for the Gain

We assume that the beam has a uniform density, $f(r) = 0$, and give asymptotic expressions for the gain in the two opposite cases of strong optical guiding and large diffraction. The beam has a radius r_b and no waveguide or cavity is present. Since there is no waveguide, the equations for δE_+ and δE_-, which were coupled through the boundary condition of the waveguide, are no longer coupled. We choose $\delta E_- = 0$ and look for the radial profile of the interacting mode δE_+. Following the analysis of Moore [3] for the cylindrical-beam FEL in the strong-pump regime and our analysis for the sheet-beam FEL in the strong-pump regime [16], we introduce the nondimensional radial coordinate,

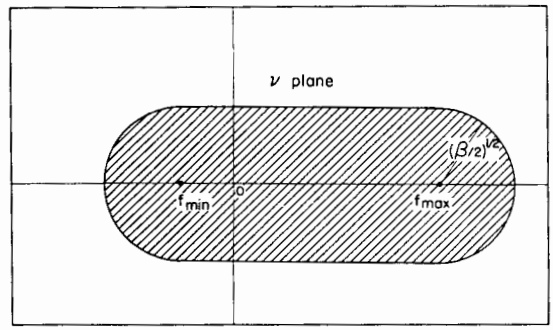

Fig. 1. The domain in the ν plane where nonreal eigenvalues are allowed.

$$\bar{r} = r/r_b \tag{89}$$

the normalized eigenvalue,

$$\phi^2 \equiv -2\frac{\omega}{c}r_b^2(\nu - \xi) \tag{90}$$

the mismatch parameter,

$$\mu = 2\frac{\omega}{c}r_b^2\xi \tag{91}$$

and the coupling parameter,

$$\alpha \equiv 2\left(\frac{\omega}{c}r_b^2\right)^2\beta = \left(\frac{\omega}{c}r_b^2\right)^2\frac{\omega_p k_w a_w^2}{\gamma^{3/2}v_z(1 + a_w^2)^{1/2}}. \tag{92}$$

The governing equation becomes:

$$\frac{1}{\bar{r}}\frac{\partial}{\partial\bar{r}}\left(\bar{r}\frac{\partial\delta E_+}{\partial\bar{r}}\right) + \left[\phi^2 - \frac{(l-1)^2}{\bar{r}^2} + \left(\frac{\alpha}{\phi^2 - \mu}\right)\right]\cdot\delta E_+ = 0, \qquad |\bar{r}| \leq 1 \tag{93a}$$

$$\frac{1}{\bar{r}}\frac{\partial}{\partial\bar{r}}\left(\bar{r}\frac{\partial\delta E_+}{\partial\bar{r}}\right) + \left[\phi^2 - \frac{(l-1)^2}{\bar{r}^2}\right]\cdot\delta E_+ = 0, \qquad |\bar{r}| > 1. \tag{93b}$$

The regular solution for $|\bar{r}| < 1$ is

$$\delta E_+ = J_{l-1}(\chi\bar{r}) \tag{94}$$

and the bounded solution for $|\bar{r}| \geq 1$ is

$$\delta E_+ = DH_{l-1}^{(1)}(\phi\bar{r}) \tag{95}$$

where

$$\chi^2 \equiv \phi^2 + \frac{\alpha}{(\phi^2 - \mu)}. \tag{96}$$

The solution (94) and (95) has the same form as in the strong-pump regime [3], [16], but the relation between χ and ϕ is different. The original eigenvalue k_z has a negative imaginary part which corresponds to a growing wave and so does ϕ^2. Therefore k_z is located in the first quadrant of the complex plane and δE_r vanishes at infinity. The continuity of the field and its derivative at $r = 1$ yields the dispersion relation:

$$\phi J_{l-1}(\chi) H_l^{(1)}(\phi) = \chi J'_{l-1}(\phi)(\chi) H_l^{(1)}(\phi) \tag{97}$$

which is identical in form to that derived by Moore [3] for the interaction in the strong-pump regime.

We first examine the case of strong optical guiding, when α is large. In that case ϕ is large and the dispersion relation is approximated as

$$i\phi J_{l-1}(\chi) = \chi J'_{l-1}(\chi) \tag{98}$$

and therefore

$$J_{l-1}(\chi) = 0 \tag{99}$$

and

$$\phi_n^2 = \left(\frac{\mu + \chi_n^2}{2}\right) + \frac{i}{2}\left[4\alpha - (\mu - \chi_n^2)\right]^{1/2}, \quad \alpha \gg 1. \tag{100}$$

Many of the modes are unstable and have about the same growth rate, which is the growth rate of the one-dimensional case. The effective filling factor is one.

The opposite case is that of large diffraction, when the coupling parameter α is small. We treat only the case $l = 1$. In that case, ϕ is very small and the relation is

$$\chi_0^2 = \frac{\alpha}{\phi_0^2} \tag{101}$$

at resonance. Also, χ is small and therefore [3], [25]

$$\frac{i\pi}{2} - \ln\left(\frac{\phi}{2}\right) - \gamma_E = \frac{2}{\chi^2} - \frac{1}{4} \tag{102}$$

where $\gamma_E = 0.577$ is the Euler–Mascheroni constant. With the former relation, we obtain

$$i\frac{\pi}{2} - \frac{1}{2}\ln\alpha + \ln(2\chi) - \gamma_E = \frac{2}{\chi} - \frac{1}{4}. \tag{103}$$

To lowest order:

$$\ln(1/\alpha) = 4/\chi_o^2$$

and

$$\phi_o^2 = \left(\frac{\alpha}{4}\right)\ln\left(\frac{1}{\alpha}\right). \tag{104}$$

In order to find the imaginary part of ϕ^2, we go to the next order. Relation (96) becomes:

$$\chi_1^2 = \phi_1^2\left(1 - \frac{\alpha}{\phi_o^4}\right) \cong -\frac{\alpha\phi_1^2}{\phi_o^4}. \tag{105}$$

Equation (103), to first order, is

$$i\frac{\pi}{2} + \ln\left\{\frac{4}{\left[\ln(1/\alpha)\right]^{1/2}}\right\} - \gamma_E = -2\frac{\chi_1^2}{\chi_o^4} - \frac{1}{4}. \tag{106}$$

Therefore,

$$\operatorname{Im}\phi^2 = -\operatorname{Im}\left(\frac{\chi_1^2\phi_o^4}{\alpha}\right) = \frac{\pi}{4}\alpha, \quad \alpha \ll 1. \tag{107}$$

Using the original variables, we express the growth rate at the two opposite limits as

$$\operatorname{Im} k_z = -\frac{(\omega_p k_w)^{1/2} a_w}{2\gamma^{3/4} v_z^{1/2}(1 + a_w^2)^{1/4}}, \quad \alpha \gg 1 \tag{108}$$

in the case of strong optical guiding, which is the one-dimensional limit, and

$$\operatorname{Im} k_z = -\frac{\pi}{8}\frac{\omega}{c} r_b^2 \frac{\omega_p k_w a_w^2}{\gamma^{3/2} v_z (1 + a_w^2)^{1/2}}, \quad \alpha \ll 1 \tag{109}$$

in the case of large diffraction. For small α the gain is increased with the increase of r_b when all other parameters are kept fixed. The increase of r_b (for constant density and increased current) increases the filling factor and therefore also the gain. When α becomes much larger than one, the filling factor approaches one. Then only the density matters and not the total current, and the gain is described by (108) with no dependence on the beam radius.

Let us now assume that the total current, defined $I = \omega_p^2 v_z r_B^2$, is kept constant, and by varying r_b we vary the density. Expressions (108) and (109) now become:

$$\operatorname{Im} k_z = -\frac{I^{1/4} k_w^{1/2} a_w}{2\gamma^{3/4} v_z^{3/4} r_b^{1/2}(1 + a_w^2)^{1/4}}, \quad \alpha \gg 1 \tag{110}$$

and

$$\operatorname{Im} k_z = -\frac{\pi}{8}\frac{\omega}{c}\frac{r_b I^{1/2} k_w a_w^2}{\gamma^{3/2} v_z^{3/2}(1 + a_w^2)^{1/2}}, \quad \alpha \ll 1. \tag{111}$$

We see that the dependence of the gain on the radius r_b is not monotonic. If one uses a beam with parameters such that $\alpha \gg 1$, and one reduces r_b, the gain becomes larger according to (110), since the density is increased. As in the one-dimensional case, the gain increases with the increase in density. However, if r_b is reduced further and α becomes smaller than one, the *decrease* in r_b causes a *decrease* in gain according to (111). This is because the decrease in the filling factor is more important for $\alpha \ll 1$

than the increase in the density. These two opposing effects of the reduction in beam dimensions are present for various regimes of operation of the FEL and in various geometries. Their relative influences vary, as has been described for the strong-pump FEL in a cylindrical geometry [3] and in a sheet-beam geometry [16]. For example, in the strong-pump FEL which employs a cylindrical beam, the gain, when diffraction is large, is proportional to $(lnr_b)^{1/2}$ and therefore keeps increasing when the beam radius is reduced. In that case the increase in gain due to the density increase is more important than the diffraction loss due to the decrease of the filling factor. A detailed comparison of the scaling of the gain for the two regimes of operation and for the two beam geometries, as well as a discussion on the limited validity of the asymptotic expressions, are given elsewhere [27].

In this section we examined the influence of the electron beam radius on the FEL interaction. In the next section we will study the effect of the waveguide radius on the FEL growth rate and wave radial profile.

VI. Numerical Examples

In this section we study numerically an FEL which employs a cylindrical electron beam in a cylindrical waveguide. We compare the growth rates and wave radial profiles for various waveguide radii. We find the wave growth rate by solving numerically the dispersion relation (69) for k_z. We find the profile of the wave field by first substituting the value of k_z into (68) and then substituting the values obtained for A_2, A_3, and A_4 into (70) and (71).

The FEL interaction within a waveguide is compared to two other cases: The FEL in the one-dimensional approximation and the FEL in the absence of a waveguide. The gain in the one-dimensional FEL is the highest, since there are no diffraction losses and the filling factor is one. The gain in the absence of a waveguide is the lowest because of diffraction losses, even though the wave modification by the electron beam (optical guiding) reduces those diffraction losses to some extent (as described in the previous section). The waveguide increases the filling factor and therefore also the gain. Reducing the waveguide radius is expected to increase the gain to a value close to the one-dimensional gain. In addition to the gain, the waveguide also modifies the wave profile. As we demonstrate below, the wave profile varies from the free-space FEL mode profile (which is composed of several vacuum waveguide modes) when a waveguide is not present or the waveguide radius is large, to a vacuum waveguide mode profile when the waveguide radius is small.

We first describe the gain calculation for the two cases of the FEL without a waveguide and the one-dimensional FEL, and the wave profile calculation when there is no waveguide. For the FEL without a waveguide we could employ the dispersion relation (97) by taking R to infinity. We prefer to analyze this case directly. The wave fields, when there is no waveguide, become:

$$\delta E_- = 0 \qquad (112a)$$

and

$$\delta E_+ = J_{l-1}(Sr), \qquad r \le r_b \qquad (112b)$$

$$\delta E_+ = AH^{(1)}_{l-1}(k_\perp r), \qquad r \ge r_b. \qquad (112c)$$

The dispersion relation is, therefore,

$$SJ'_{l-1}(Sr_b)H^{(1)}_{l-1}(k_\perp r_b) = k_\perp H^{(1)\partial}_{l-1}(k_\perp r_b)J_{l-1}(Sr_b). \qquad (113)$$

We find k_z by solving (113); we then calculate A $(= J_{l-1}(Sr_b)/H^{(1)}_{l-1}(k_\perp r_b))$, and using (112) we find the fields.

We compare our calculated growth rate with the growth rate of the one-dimensional FEL. In the one-dimensional case the dispersion relation is

$$S^2 \equiv \omega^2 - k_z^2 - \frac{\omega}{c}Q = 0. \qquad (114)$$

In the numerical examples the beam radius r_b is 0.2 cm, the beam energy γ is 2.5, and the current density 2 kA/cm^2. The wiggler parameter a_w is 0.42 and the wiggler wavenumber k_w is 3.7 cm^{-1}. The azimuthal number l is 1.

Fig. 2 shows the maximal growth rate and the frequency at the maximal growth rate (the resonant frequency) as a function of the waveguide radius R. For smaller waveguide radii the resonant frequency is lower. When R is reduced, $k_\perp$ is increased and the gain is reduced [28]. However, the reduction of R increases the filling factor and as a result the gain is increased. From Fig. 2 it is clear that the increase in the filling factor dominates. This is true as long as R is not too small, in which case the gain vanishes. The two Doppler-upshifted and -downshifted resonant frequencies are approximately:

$$\omega_{1,2} = \frac{k_w v_z}{(1 - v_z^2/c^2)}\left\{1 \pm \left[\frac{v_z^2}{c^2} - \frac{k_\perp^2}{k_w^2}\left(1 - \frac{v_z^2}{c^2}\right)\right]^{1/2}\right\}. \qquad (115)$$

When R is small enough (and $k_\perp$ is large enough) the term in the square brackets becomes negative and the FEL interaction disappears. This is reflected in the abrupt fall of the growth rate for $R < 0.275$ cm. The maximal growth rate of the one-dimensional FEL (A in Fig. 2) is 0.204 cm^{-1}, and the frequency at which that growth rate is maximal (B in Fig. 2) is $\omega/c = 30.8$ cm^{-1}. The wavenumber k_z corresponding to a maximal growth rate when a waveguide is not present is $29.085 - i0.0485$ cm^{-1} (the growth rate is denoted in Fig. 2 as C), and the frequency at which the growth rate is maximal is $\omega/c = 29.9$ cm^{-1} (D in Fig. 2).

Figs. 3–10 illustrate the somewhat competing effects of the waveguide and FEL interaction on the profiles of the wave-field components $\sqrt{2}|\delta E_+|$, $\sqrt{2}|\delta E_-|$, $|\delta E_z|$, and $|\delta B_z|$. First, Figs. 3 and 4 show these wave components of the vacuum waveguide modes TE_{11} and TM_{11}. Next, Fig. 5 shows the free-space FEL mode for the case in

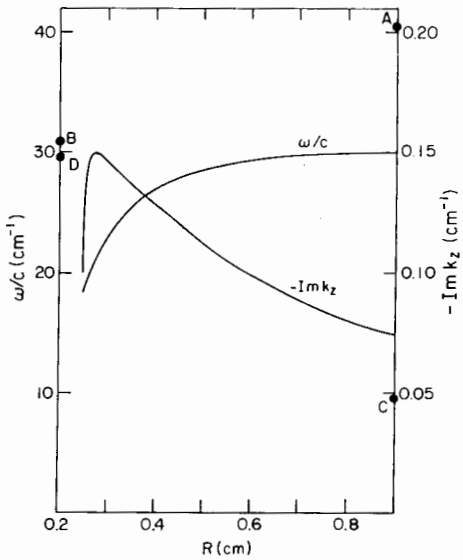

Fig. 2. The maximal growth rate ($-Imk_z$) and frequency (ω/c) at which the growth rate is maximal as a function of the waveguide radius R. Also denoted are Imk_z and ω/c for the maximal growth rate for the one-dimensional FEL (A and B) and for an FEL without a waveguide (C and D). The parameters are: $a_w = 0.42$, $k_w = 3.7$ cm^{-1}, $\gamma = 2.5$, and current density = 2 kA/cm^2. The azimuthal wavenumber l is 1. The beam radius is $r_b = 0.2$ cm.

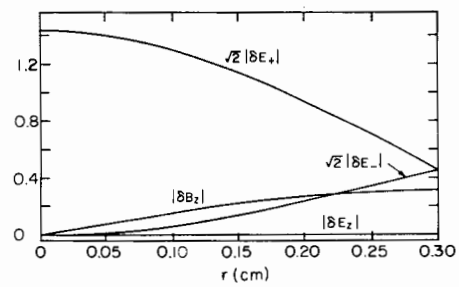

Fig. 3. The absolute values of the wave components $\sqrt{2}|\delta E_+|$, $\sqrt{2}|\delta E_-|$, $|\delta E_z|$, and $|\delta B_z|$ of the vacuum TE_{11} mode. The parameters are: $\omega/c = 23.0$ cm^{-1}, and $R = 0.3$ cm.

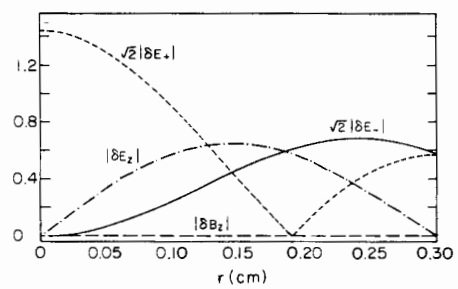

Fig. 4. The absolute values of the wave components $\sqrt{2}|\delta E_+|$, $\sqrt{2}|\delta E_-|$, $|\delta E_z|$, and $|\delta B_z|$ of the vacuum TM_{11} mode. The parameters are: $\omega/c = 23.0$ cm^{-1}, and $R = 0.3$ cm.

which no waveguide is present. The mode shown is the most unstable FEL mode, for the frequency and growth rate given in Fig. 2 (D and C). By comparing the profiles in Figs. 3 and 4 versus those in Fig. 5, we observe the differences between the vacuum waveguide modes and the free-space FEL mode. The vacuum waveguide modes are either TE or TM modes and the component δE_- is not zero. The components $|\delta E_z|$ and $|\delta B_z|$ of the FEL mode

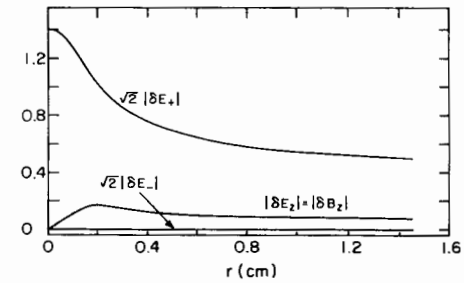

Fig. 5. The absolute values of the wave components of the free-space FEL mode. No waveguide is present. The parameters are the same as those of Fig. 2. Also: $k_z = 29.085 - i0.0485$ cm^{-1}, and $\omega/c = 29.9$ cm^{-1}.

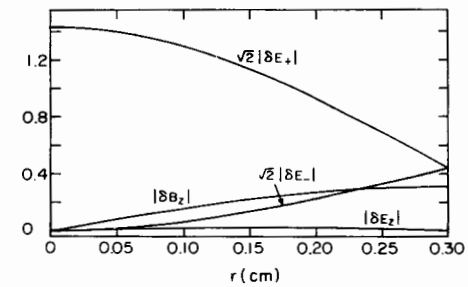

Fig. 6. The absolute values of the wave components of the FEL mode for $R = 0.3$ cm. The other parameters are as in Fig. 2. Also: $k_z = 22.2 - i0.146$ cm^{-1}, and $\omega/c = 23.0$ cm^{-1}.

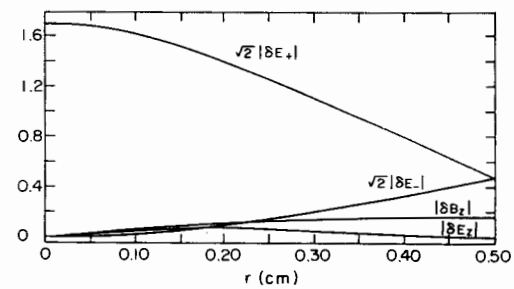

Fig. 7. The absolute values of the wave components of the FEL mode for $R = 0.5$ cm. The other parameters are as in Fig. 2. Also: $k_z = 28.08 - i0.112$ cm^{-1}, and $\omega/c = 28.3$ cm^{-1}.

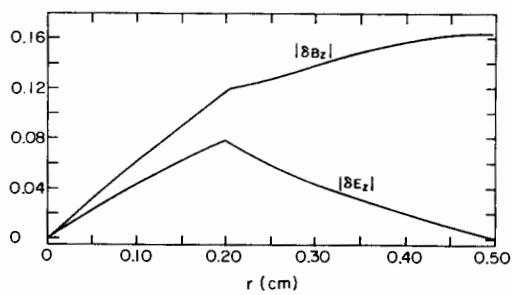

Fig. 8. The absolute values of the longitudinal components $|\delta E_z|$ and $|\delta B_z|$ of the FEL mode of Fig. 7.

are, in contrast, equal. The FEL mode is neither a TE nor TM mode, but rather is of a mixed type. Also, the left-hand polarized wave δE_- of the FEL mode is zero.

When an FEL operates within a waveguide the wave profile is different from both the vacuum waveguide modes (Figs. 3 and 4) and the free-space FEL mode (Fig. 5). When the waveguide radius is small, the FEL mode re-

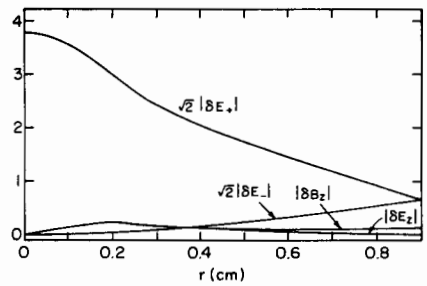

Fig. 9. The absolute values of the wave components of the FEL mode for $R = 0.9$ cm. The other parameters are as in Fig. 2. Also: $k_z = 29.99 - i0.0749$ cm^{-1}, and $\omega/c = 29.9$ cm^{-1}.

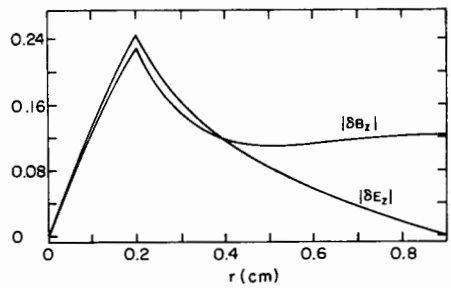

Fig. 10. The absolute values of the longitudinal components of the FEL mode of Fig. 9.

sembles a vacuum waveguide mode. Fig. 6 shows the most unstable FEL mode for $R = 0.3$ cm. Its profile is very similar to the vacuum TE_{11} mode. The component δE_z is almost zero, while δB_z is similar to δB_z of the vacuum TE_{11} mode. When R is 0.5 cm, the wave profiles have some similarity to the free-space FEL mode as well. The left-hand polarized wave δE_- is smaller and δE_z is finite (Fig. 7). The longitudinal components $|\delta B_z|$ and $|\delta E_z|$ for $R = 0.5$ cm are shown also in Fig. 8. When the waveguide radius is even larger ($R = 0.9$ cm), the wave profile is modified considerably by the FEL interaction (Fig. 9). It strongly resembles the free-space FEL mode. The component δE_- is very small. The longitudinal components $|\delta E_z|$ and $|\delta B_z|$ are nearly identical (Fig. 10), as in the free-space FEL mode (Fig. 5), and their magnitudes are different only near the waveguide wall.

The reason for the above influence of the waveguide radius on the FEL mode is the following: When R is small the difference between the values of $k_\perp$ for neighboring vacuum waveguide modes is relatively large. The change in $k_\perp$ due to the FEL interaction is smaller than that difference and therefore the FEL modes are only slightly modified from the vacuum waveguide modes. On the other hand, when R is large that difference becomes small, and the FEL mode is described as a coupling of several vacuum waveguide modes. The FEL mode is then significantly different from each individual vacuum-waveguide mode. The FEL experiments at Columbia University included both experiments with an FEL mode very similar to a vacuum waveguide mode [29] (R was 0.32 cm) and experiments where the FEL mode was significantly different from any particular vacuum waveguide mode [23] (R was 0.9 cm). The beam and wiggler parameters of our numerical examples are similar to those in the Columbia experiments, although a_w in our example is 0.42, while at the Columbia FEL it was smaller, about 0.3.

The wave profile modification, and thus its greater confinement to the electron beam volume, results in a higher gain due to the enhanced effective filling factor. On the other hand, the FEL interaction affects the purity of the vacuum waveguide modes. These two effects are clearly demonstrated in this paper. The present formalism can, therefore, be used to calculate the expected gain, wave profile, and mode structure in the linear regime in planning FEL experiments.

Acknowledgment

The author benefited from useful discussions with A. Bhattacharjee, T. C. Marshall, E. Jerby, A. Gover, and J. S. Wurtele.

References

[1] T. C. Marshall, *Free Electron Lasers*. New York: Macmillan, 1985, and references therein.
[2] E. T. Scharlemann, A. M. Sessler, and J. S. Wurtele, "Optical guiding in a free-electron laser," *Phys. Rev. Lett.*, vol. 54, pp. 1925–1928, 1985.
[3] G. T. Moore, "The high-gain regime of the free-electron laser," *Nucl. Instrum. Methods*, vol. A239, pp. 19–28, 1985.
[4] P. Luchini and S. Solimeno, "Optical guiding in an FEL," *Nucl. Instrum. Methods*, vol. A250, pp. 413–417, 1985.
[5] M. Xie and D. A. G. Deacon, "Theoretical study of FEL active guiding in the small signal regime," *Nucl. Instrum. Methods*, vol. A250, pp. 426–431, 1985.
[6] K. J. Kim, "Three-dimensional analysis of coherent amplification and self-amplified spontaneous emission in free-electron lasers," *Phys. Rev. Lett.*, vol. 57, pp. 1871–1874, 1986.
[7] P. Sprangle, A. Ting, and C. M. Tang, "Radiation focusing and guiding with application to the free electron laser," *Phys. Rev. Lett.*, vol. 59, pp. 202–205, 1987.
[8] S. Krinsky and L. H. Hu, "Output power in guided modes for amplified spontaneous emission in a single-pass free-electron laser," *Phys. Rev.*, vol. A35, pp. 3406–3423, 1987.
[9] B. Hafizi, P. Sprangle, and A. Ting, "Optical gain, phase shift, and profile in free-electron lasers," *Phys. Rev.*, vol. A36, pp. 1739–1746, 1987.
[10] A. Fruchtman, "A thick beam free-electron laser," *Phys. Fluids*, vol. 30, pp. 2496–2503, 1987.
[11] S. Y. Cai, A. Bhattacharjee, and T. C. Marshall, "Optical guiding in a Raman free electron laser," *IEEE J. Quantum Electron.*, vol. QE-23, pp. 1651–1656, 1987.
[12] E. Jerby and A. Gover, "A linear three-dimensional model for free-electron laser amplifiers," *Nucl. Instrum. Methods*, vol. A272, pp. 380–385, 1988.
[13] H. P. Freund, H. Bluem, and C. L. Chang, "Three-dimensional simulation of free electron lasers with planar wigglers," *Nucl. Instrum. Methods*, vol. A272, pp. 556–563, 1988.
[14] M. Xie, D. A. G. Deacon, and J. M. J. Madey, "The guided mode expansion in free electron lasers," *Nucl. Instrum. Methods*, vol. A272, pp. 528–531, 1988.
[15] L.-H. Yu and S. Krinsky, "Gain reduction due to betatron oscillations in a free electron laser," *Phys. Lett.*, vol. A129, pp. 463–469, 1988.
[16] A. Fruchtman, "Optical guiding in a sheet-beam free-electron laser," *Phys. Rev.*, vol. A37, pp. 2989–2999, 1988.
[17] A. Fruchtman, "High density thick-beam free-electron laser," *Phys. Rev.*, vol. A37, pp. 4259–4264, 1988.
[18] A. Fruchtman and H. Weitzner, "Raman free-electron laser with transvers density gradients," *Phys. Rev.*, vol. A39, pp. 658–667, 1989.
[19] T. M. Antonsen, Jr., and P. E. Latham, "Linear theory of a sheet beam free electron laser," *Phys. Fluids*, vol. 31, pp. 3379–3386, 1988.

[20] E. Jerby and A. Gover, "Wave profile modification in free-electron lasers: Space-charge transverse fields and optical guiding," *Phys. Rev. Lett.*, vol. 63, pp. 864–867, 1989.
[21] R. W. Warren and B. D. McVey, "Bending and focusing effects in an FEL oscillator I: Simple models," *Nucl. Instrum. Methods*, vol. A259, pp. 154–157, 1987.
[22] F. Hartemann, K. Xu, G. Bekefi, J. S. Wurtele, and J. Fajans, "Wave-profile modification (optical guiding) induced by the free-electron laser interaction," *Phys. Rev. Lett.*, vol. 59, pp. 1177–1180, 1987.
[23] A. Bhattacharjee, S. Y. Cai, S. P. Chang, J. W. Dodd, and T. C. Marshall, "Observations of optical guiding in a Raman free-electron laser," *Phys. Rev. Lett.*, vol. 60, pp. 1254–1257, 1988.
[24] H. P. Freund and A. K. Ganguly, "Nonlinear analysis of efficiency enhancement in free-electron-laser amplifiers," *Phys. Rev.*, vol. A33, pp. 1060–1072, 1986.
[25] M. Abramowitz and I. A. Stegun, *Handbook of Mathematical Functions*. New York: Dover, 1965, p. 360.
[26] A. Bhattacharjee *et al.*, "Theory and observation of optical guiding in a free electron laser," *Phys. Rev.*, vol. A40, pp. 5081–5091, 1989.
[27] A. Fruchtman, "Gain reduction in FELs due to diffraction losses" *Nucl. Instrum. Methods*, vol. A285, pp. 122–127, 1989.
[28] A. Friedman, A. Gover, G. Kurizki, S. Ruschin, and A. Yariv, "Spontaneous and stimulated emission from quasi-free electrons," *Rev. Mod. Phys.*, vol. 60, pp. 471–535, 1988.
[29] J. Masud, T. C. Marshall, S. P. Schlesinger, and F. G. Yee, "Regenerative gain in a Raman free-electron laser oscillator," *IEEE J. Quantum Electron.*, vol. 23, pp. 1594–1604, 1987.
[30] F. Hartemann, G. Mourier, and R. C. Davidson, "Anomalous (stimulated) refraction induced by the free-electron laser interaction," Plasma Fusion Ctr., MIT, Cambridge, MA, PFC Rep. No. PFC/JA-89-51.

*

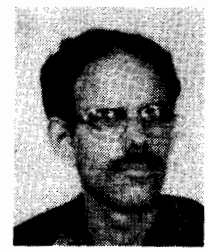

Amnon Fruchtman was born in Rehovot, Israel, on August 21, 1952. He received the B.Sc. (physics) degree in 1973 from Tel Aviv University, the M.Sc. degree in 1978, and the Ph.D. degree in plasma physics, from the Hebrew University of Jerusalem in 1983, for suggesting and analyzing the wiggler-free free electron laser.

As a Chaim Weizmann Postdoctoral Fellow in 1983–1985 and as a Research Scientist in 1985–1986, he worked at the Courant Institute, New York University, on wave propagation and the RF heating in plasmas. In October 1986 he joined the Weizmann Institute of Science, Rehovot, Israel, where he is now a Senior Scientist. His research topics include various aspects of plasma physics, such as magnetic field–plasma interactions, plasma waves and instabilities, ion diodes, plasma switches and pinches, and free electron lasers.

Dr. Fruchtman is a member of the American Physical Society.